Title

Cerebrospinal fluid metabolomics implicate bioenergetic adaptation as a neural mechanism regulating shifts in cognitive states of HIV-infected patients

Journal

AIDS, 29(5)

ISSN

0269-9370

Authors

Dickens, Alex M

Anthony, Daniel C

Deutsch, Reena

et al.

Publication Date

2015-03-13

DOI

10.1097/qad.0000000000000580

Peer reviewed

Published in final edited form as:
AIDS. 2015 March 13; 29(5): 559–569. doi:10.1097/QAD.0000000000000580.

Cerebrospinal fluid metabolomics implicate bioenergetic adaptation as a neural mechanism regulating shifts in cognitive states of HIV-infected patients

Alex M. Dickens[a,b], **Daniel C. Anthony**[a], **Reena Deutsch**[d], **Michelle M. Mielke**[e], **Timothy D.W. Claridge**[f], **Igor Grant**[d], **Donald Franklin**[d], **Debra Rosario**[d], **Thomas Marcotte**[d], **Scott Letendre**[d], **Justin C. McArthur**[c], and **Norman J. Haughey**[b,c]

[a]Department of Pharmacology, University of Oxford, Oxford, UK [b]Department of Neurology, Johns Hopkins University, Baltimore, Maryland [c]Department of Psychiatry, Johns Hopkins University, Baltimore, Maryland [d]HIV Neurobehavioral Research Program and Department of Psychiatry, School of Medicine, University of California, San Diego, La Jolla, California [e]Division of Epidemiology, Department of Health Sciences Research and Department of Neurology College of Medicine, Mayo Clinic, Rochester, Minnesota, USA [f]Department of Chemistry, University of Oxford, UK

Abstract

Objectives—To identify prognostic surrogate markers for change in cognitive states of HIV-infected patients.

Design—Longitudinal cerebrospinal fluid (CSF) samples were collected from 98 HIV+ patients identified by temporal change in cognitive states classified as normal, stably impaired, improving and worsening.

Methods—The metabolic composition of CSF was analysed using ^{1}HNMR spectroscopy that focused on energy metabolites. Metabolic biomarkers for cognitive states were identified using multivariate partial least squares regression modelling of the acquired spectra, combined with nonparametric analyses of metabolites with clinical features.

Results—Multivariate modelling and cross-validated recursive partitioning identified several energy metabolites that, when combined with clinical variables, classified patients based on change in neurocognitive states. Prognostic identification for worsening was achieved with four features that included no change in a detectable plasma viral load, elevated citrate and acetate; decreased creatine, to produce a model with a predictive accuracy of 92%, sensitivity of 88% and

Correspondence to Norman J. Haughey, Johns Hopkins University School of Medicine, Departments of Neurology and Psychiatry, Pathology 517, 600 North Wolfe Street, Baltimore, MD 21287, USA. nhaughe1@jhmi.edu.

Author contributions: N.J.H., J.C.M. and D.C.A. conceived and designed the study. A.M.D. and T.D.W.C. performed the NMR experiments and subsequent analysis. R.D. performed all the recursive partitioning analysis. M.M.M. performed all the linear regression analysis. D.F., D.R., I.G., T.M. and S.L. classified the patients as part of the ARC biomarker study.

Conflicts of interest
None declared.

96% specificity. Prognosis for improvement contained seven features that included first visit age less than 47 years, new or continued use of antiretrovirals, elevated glutamine and glucose; decreased *myo*-inositol, β-glucose and creatinine to generate a model with a predictive accuracy of 92%, sensitivity of 100% and specificity of 84%.

Conclusion—These CSF metabolic results suggest that worsening cognitive status in HIV-infected patients is associated with increased aerobic glycolysis, and improvements in cognitive status are associated with a shift to anaerobic glycolysis. Dietary, lifestyle and pharmacologic interventions that promote anaerobic glycolysis could protect the brain in setting of HIV infection with combined antiretroviral therapy.

Keywords

brain energy metabolism; HIV; HIV-associated neurocognitive disorders; metabolomics

Introduction

Although combined antiretroviral therapy (cART) has become a highly effective tool in controlling replication of the HIV, cART is not completely effective in suppressing the neurological complications of HIV infection [1–6]. Although some cases of cognitive impairment can be attributed to cART failure, many individuals develop HIV-associated neurocognitive disorders (HAND) with stable cART, low levels or undetectable viral load, and $CD4^+$ cell counts in the normal range [7]. Understanding the aetiologic basis of HAND in this population is critically important to the development of adjunctive therapies to protect and restore the brain in HIV-infected individuals.

Several lines of evidence suggest that HIV infection and cART are each associated with disturbances in peripheral and central bioenergetics disturbances [8–14]. Whereas brain imaging emphasizes the importance of metabolic abnormalities in HIV-infected patients, the underlying bioenergetic pathways modified by infection are not understood. In this study, we identify specific metabolite changes in cerebrospinal fluid (CSF) of HIV-infected patients, and use partial least squares discriminant analysis (PLS-DA) modelling with nonparametric statistical approaches to determine the relationship of these changes to the longitudinal trajectories of neurocognitive function in HIV-infected patients.

Materials and methods

Patients and sample collection

Ninety-nine CSF samples from the Central Nervous System HIV Anti-Retroviral Therapy Effects Research study were selected based on a case review of approximately 3500 clinical visits from 430 study participants as recently described [15]. Patients met the following criteria: three consecutive visits with complete clinical and neuropsychological data, stable cART for at least 3 months before the first visit and throughout the duration of this study period (a single drug modification in cART was allowed if within the same drug class). Based on temporal change in neurocognitive functioning, patients were grouped as normal (n = 25), improving (n = 23), worsening (n = 25) and stably impaired (n = 26). See [15] for a detailed description of criteria in neurocognitive status. Group demographics were similar,

as were HIV duration, hepatitis C virus status, nadir $CD4^+$, plasma and CSF viral load. There were significant group differences in current $CD4^+$ and CSF storage time (SI1). Metabolite analysis was conducted using CSF from the first two visits, and neurocognitive data from the third visit were used to validate the trajectory of change in cognitive functioning.

Neurocognitive test battery

The following seven cognitive domains were evaluated: executive function [16,17], learning and delayed recall [18,19], working memory [20,21], verbal fluency [16], speed of information processing [17,20,21] and motor skills [22]. Deficit scores were calculated as previously described [15].

NMR spectroscopy

CSF samples (50 μl each) were placed in a 5mm NMR tube and diluted to a final volume of 600 μl with phosphate buffer (0.2 mol/l Na_2HPO_4/0.04 NaH_2PO_4, pH 7.4, 0.1% sodium azide, 0.8% sodium chloride) in D_2O containing 1 mmol/l TSP (3-trimethylsilyl-1-[2,2,3,3,-$^2H_4$] propionate) as an internal standard. ^1H NMR spectra were acquired from each sample using a 16.4 T NMR (700MHz ^1H) system (Bruker Avance III equipped with a ^1H TCI cryoprobe). For all samples a one-dimensional NOESY presaturation sequence, with solvent presaturation during the relaxation delay (2 s) and mixing time (10 ms), was used with 32 scans. All one-dimensional spectra were automatically baseline corrected using a 0th order polynomial (Topspin 3.0). Two dimensional ^1H NMR spectra were acquired from a sample within each group to assist with metabolite identification. The two-dimensional correlation spectroscopy (COSY) spectra were acquired on the same spectrometer as the one-dimensional NMR spectra. The COSY spectra were acquired with 1.5 s solvent presaturation, a spectral width of 10 ppm (7002 Hz), and 32 transients per t_1 increment for 256 increments. All NMR experiments were acquired at 293K.

Spectra processing

The one-dimensional ^1H spectra were subdivided into 0.02 ppm regions (δ = midpoint of integral region) and integrated using ACD/SpecManager version 12 (Advanced Chemistry Development, UK). Thus, spectra were reduced to 435 independent variables between 0.20–4.30 and 5.00–9.60 ppm. The region between 4.30 and 5.00 ppm was omitted because of spectrum distortion arising from the water suppression at 4.7 ppm. The buckets containing only baseline noise were removed from the analysis. Using these criteria, 66 buckets were identified that contained ^1H NMR resonances. These buckets were 1.32..1.34, 1.46..1.48, 1.90..1.92, 2.10..2.16, 2.36..2.70, 3.02..3.06, 3.22..3.64, 3.68..4.14, 5.22..5.24 (including all 0.02 ppm buckets between the two values). Baseline noise was removed by visual inspection of the spectra (SI2 A). The spectra were overlaid (Topspin 2.1, Bruker), and the regions containing peaks visible over the background noise were selected. All data were scaled using the Pareto variance to suppress noise. Subsequently, statistical pattern recognition was applied to the spectra to differentiate between CSF samples obtained from patients with different cognitive states. The metabolites were identified using a combination of two-dimensional COSY spectroscopy (SI2 B) and reference to the Human Metabolome database [23–25].

Linear regression analysis

Associations between each metabolite and domain-specific cognitive performance scores at baseline were determined using linear regression controlling for age, education, nadir $CD4^+$ and storage time. In these analyses, we included all individuals regardless of longitudinal group assignment. If the metabolite signal appeared in multiple bins within the spectra, the bin with the largest integral value was selected for analysis. The *a priori P* value was set at $P<0.05$. All tests were two sided. These analyses were performed using Stata 12 (StataCorp: Stata Statistical Software, College Station, Texas, USA).

Multivariate analysis

For group comparisons, PLS-DA and orthogonal partial least squares discriminant analysis (OPLS-DA) models were derived that best explained the differences between the four cognitive groups (SIMCA P+ 12.0, Umetrics, Sweden). We determined the predictive value of the models using the q^2 value derived from a stepwise cross-validation of the model. In this validation, a fraction of the samples are removed, the model is rebuilt and the new model is used to predict the class of the removed samples. Specifically, q^2 represents the predicted residual sum of squares divided by the initial sum of squares and subtracted from 1. A value of q^2 more than 0 means that the model is predictive and a value of more than 0.4 is typically used as the threshold for significance in biological modelling [26]. Model validation was also carried out within SIMCA using a pseudo-Monte Carlo method in which we built 100 models with the samples assigned to random groups. The goodness-of-fit of each of these randomly permuted models was compared with the fit for the models produced using experimentally defined groups. Only models in which the genuine q^2 value was higher than 95% of the randomly generated q^2 values were considered predictive.

Risk estimation analysis

Decision models were developed by recursive partitioning [27]. Metabolites and clinical variables measured at the first visit and, in separate analyses, baseline metabolites combined with change between visits for clinical variables were used as potential classifying criteria to assign groups based on temporal change in cognitive status. Five-fold cross-validation guarded against overfitting models to the sample. Initially, a full model was generated to achieve the best fit. Proceeding through paths of this decision model, if a variable previously entered into the model was followed by subsequent inclusion of the same variable with a different decision path, the subsequent variable was removed, and splitting of the tree was continued until no further additions improved the model. The resultant tree was then ‘pruned’ to reduce complexity until no further reduction was made without reaching a higher misclassification rate than the prespecified limit of 10% if possible. The pruning ensured that as few metabolites and clinical variables as possible would be needed to achieve the prespecified levels of accuracy. Confusion matrices were generated to tabulate the number of patients correctly and incorrectly classified to each group.

Results

Cross-sectional associations between energy metabolites and domain-specific cognitive performance at baseline

^{1}H NMR spectroscopy of CSF identified 14 energy metabolites in CSF (SI2 A-B and SI3 for full assignments). At baseline, increased CSF levels of pyroglutamate, citric acid, creatine and alanine were significantly associated with deficits in global cognitive function. All other energy metabolites identified showed similar trends, with the exception of glutamine (Table 1). To identify components of the global deficit score responsible for these associations, we grouped metabolites according to domain-specific cognitive scores. Deficits in executive functioning were associated with higher CSF concentrations of lactate, pyroglutamate, citrate and creatine. Verbal learning was negatively associated with higher pyroglutamate. Impairments in delayed recall were associated with higher pyroglutamate, creatine *myo*-inositol, alanine and acetate. Impairments in motor function were associated with higher concentrations of lactate, citrate, creatinine, *myo*-inositol, alanine and acetate. Verbal memory, speed of information processing and working memory were not associated with any energy metabolites (Table 1). As negative associations of these energy metabolites with cognitive function could represent a compensatory response, or may be causal of impairments in cognitive processing, we next sought to determine how energetic demand varied in association with changes in cognitive status.

Longitudinal multivariate modelling

Initial PLS-DA models did not reveal cross-sectional separations between improving, worsening, normal or impaired groups at baseline. However, visual separations were observed in the PLS-DA models between baseline and follow-up samples for each neurocognitive group (Fig. 1a). Each of these models was predictive with q^2 values equal to 0.61 (normal), 0.84 (stably impaired), 0.47 (worsening) and 0.52 (improving). Identification of the specific metabolites that drove group differences in this first model was not possible because of interference from unidentified nondisease-related factors. We generated OPLS-DA models to remove these factors from the models.

Examination of the S plots generated by OPLS-DA modelling identified several metabolites that drove longitudinal separations between neurocognitive groups. The results from these unsupervised analyses identified several TCA cycle energy metabolites and essential amino acids that were differentially regulated by neurocognitive status. We separated these into metabolites decreased (Fig. 1b), and increased at baseline relative to follow-up (Fig. 1c). Normal and worsening groups both had decreased levels of citric acid and pyroglutamic acid and increased glutamine and lactic acid at follow-up compared with baseline. Stably impaired and improved groups both showed decreased glutamine and glucose with increased citric acid, pyroglutamic acid and lactic acid at follow-up compared with baseline. CSF levels of *myo*-inositol increased in the stably impaired group. To better define these initial separations, we next used recursive partitioning and incorporated clinical variables to identify the group of variables that could potentially be used as prognostic indicators for changes in cognitive status.

Prognostic indicators for worsening and improving neurocognitive status

A prognostic identification for worsening contained seven features that included four clinical measures (nadir $CD4^+$<322, current $CD4^+$<136, detectable plasma viral load and off antiretrovirals) in addition to three metabolites (elevated glutamine and creatinine; decreased citrate) (Fig. 2a), to achieve an error rate of 14% (additional modifications in modelling did not lower the error rate) with a sensitivity of 96%, and specificity of 76% (Fig. 2a insert). Prognosis for improvement consisted of seven features that included three clinical factors (current $CD4^+$<176, detectable plasma viral load, and hepatitis C virus negative), combined with four metabolites (elevated lactate and glutamine decreased glucose and acetate) (Fig. 2b) to produce a less than 10% error rate with 87% sensitivity and 96% specificity (Fig. 2b insert). As current disease status could confound these baseline prognostic indicators (i.e. by definition, those who improved most over time were the most impaired at baseline), we next analyzed change in individual clinical measures from baseline to follow-up.

Incorporating the trajectory of change in defined clinical measures with baseline metabolic features reduced model complexity

Incorporating change of clinical status into recursive partitioning reduced the complexity of the decision trees. Prognostic identification for worsening was achieved with four features that included one clinical measure (no change in a detectable plasma viral load), and three metabolites (elevated citrate and acetate; decreased creatine) (Fig. 3a), to produce a model with a predictive accuracy of 92%, 88% sensitivity and 96% specificity (Fig. 3a insert). Prognosis for improvement contained seven features that included two clinical measures (first visit age less than 47 years, new or continued use of antiretrovirals) (Fig. 3b), and five metabolites (elevated glutamine and glucose; decreased *myo*-inositol, β-glucose and creatinine) to generate a model with a predictive accuracy of 92%, a sensitivity of 100% and specificity of 84% (Fig. 3b insert).

Discussion

This study demonstrates that CSF energy metabolites in HIV-infected patients are related to temporal changes in neurocognitive state. Overall, markers of increased aerobic metabolism were associated with worsening cognitive function, and markers of increased anaerobic metabolism tended to be associated with improving cognitive status in HIV-infected patients. Throughout the discussion, the reader is encouraged to refer to the decision trees for clarity, as each of the risk factors described depends on the value of other risk factors for inclusion into a particular group.

Worsening cognitive status

The brain is especially sensitive to alterations in energy substrate availability [28]. In HIV-infected patients with declining neurocognitive status, we found evidence for increased glycolysis (Fig. 4). This is likely related to altered glial cell function as the conversion of acetate to acetyl-CoA occurs almost exclusively within the glial cells in the central nervous system [29,30], and carbon labelling of acetate in human studies has shown this anion to be readily converted to glutamate [29]. Citrate accumulates when the glycolytic rate exceeds TCA cycle activity, and has been noted a key metabolic feature of some astrocytomas [31].

When the citric acid cycle is saturated, citrate concentrations increase and directly inhibit phosphofructokinase, a rate-limiting enzyme of glycolysis. Among possible explanations, the two most likely are that there is an excessive glycolytic rate in patients with cognitive worsening or that there are deficiencies in the TCA cycle that slow citrate metabolism. However, the decrease of CSF creatine in patients with worsening cognitive status suggests that high brain energy demand may drive an increased glycolytic rate in patients with worsening cognitive status. Creatine is tightly linked to oxidative metabolism and a critical source of phosphate when energy demand is high [32]. Energy production from phosphocreatine is regulated by the creatine phosphokinase system which catalyses a reversible reaction that uses ATP to create phosphocreatine or liberates a high-energy phosphate from phosphocreatine to create ATP [33]. One function of this energy source is to maintain ATP at a steady state by buffering excess ATP, and rapidly producing ATP as required. Elevated creatine and citrate in the CSF of HIV-infected patients with worsening cognitive function provides additional evidence that suggests an increased rate of glycolysis in these patients. Although these data do not provide the means to identify the underlying pathology driving this increase in energy demand, HIV is known to productively infect microglia [34–36], with a more restrictive infection of astrocytes [37–46]. Thus, we speculate that our CSF metabolic results may reflect the glial response to infection. However, we cannot rule out possible contributions of increased neuronal glycolysis which may directly contribute to the production of pyruvate for TCA metabolism [47].

Incorporating clinical findings and energy metabolites into recursive partitioning models revealed important contributions of nadir $CD4^+$, current $CD4^+$, plasma viral load and antiretroviral status to worsening cognitive status. A nadir $CD4^+$ less than 322, current $CD4^+$ at least 136 and undetectable viral load were associated with worsening of cognitive status if CSF citrate was low or creatinine was high. However, if the same cut-off values for nadir and current $CD4^+$ were applied to patients with a detectable plasma viral load, then off antiretrovirals or elevated CSF glutamine content were associated with a worsening phenotype. Thus, nadir and current $CD4^+$ cell counts contributed to prognosis for worsening in all patients (consistent with previous studies [48,49]), but the metabolic features associated with worsening were dependent on a detectable or undetectable viral load. This combined modelling approach identified worsening patients with a predictive accuracy of 86%, a sensitivity of 96% and specificity of 76%.

Improving cognitive status

Our CSF metabolic results suggest that adaptation to anaerobic glycolysis was associated with improving cognitive status in HIV-infected patients (Fig. 4). Decreased glucose and acetate with increased lactate were associated with improving cognitive status, and is consistent with a shift from aerobic to anaerobic glycolysis (fuelled by lactate). Neurons use both glucose and lactate as an energy source. Whether glucose or lactate is the primary energy source for neurons has been long debated [50–52]. Lactate is preferentially produced by astrocytes, and is provided to neurons through the astrocyte to neuron lactate shuttle [53,54]. This transfer of lactate to neurons is upregulated during periods of increased synaptic activity [55], or when glucose levels are low [56]. Lactate has been shown to promote synaptic plasticity through induction of plasticity-related genes such as Arc, c-Fos,

and Zif268 [57], and promotes norepinephrine release from locus coeruleus neurons [58]. Thus, our current findings suggest that increased lactate production may be at least partially responsible for improvements of cognitive function in HIV-infected patients.

We also observed elevated CSF levels of glutamine in the improving group, suggesting that an increased buffering of glutamate may also contribute to cognitive improvement. Glutamine is a trophic amino acid produced largely in astrocytes by a glutamine synthase mediated conversion of glutamate to glutamine. HIV infection, encephalitis, HIV-gp120, Tat, tumour necrosis factor α and interleukin-1β impair glutamate uptake [59,60], and gp120 is known to reduce glutamine levels and survival of cultured astrocytes [61]. Free radical scavenging with *N*-acetylcysteine protects astrocytes from gp120 and increases glutamine concentrations [61]. These data suggest that improvements in glial energetics may facilitate recovery of cognitive function by increasing uptake and conversion of glutamate to glutamine in patients with improving cognitive function.

Incorporating clinical data with CSF metabolic results better separated patients with improving cognition and those stably impaired. However, baseline clinical variables were less easily interpreted in this group because most patients in the improving category were impaired at baseline. By incorporating longitudinal changes into the modelling, we found that *myo*-inositol was a critical branch point where lower levels were associated with improving cognitive function in persons less than 47 years of age, or with higher glutamine levels. However, if *myo*-inositol was high, then considerably more variables were required including higher glucose, or lower β-glucose and creatine, with consistent or new antiretroviral use for association with improving cognitive function. *myo*-Inositol is widely considered to be a marker of glial activation, and was found to be elevated in MRS studies of HIV-infected patients with cognitive impairment [62–64] and in CSF [65]. These data suggest that decreased glial activation is most often associated with improving cognitive status, but also that high *myo*-inositol may associate with improving cognition in a small number of patients (four of 48) if glucose is high or creatine is low in patients with new or stable antiretroviral use. As *myo*-inositol is produced from glucose (via glucose 6-phosphate), these data suggest that elevated glucose may promote the formation of *myo*-inositol. As *myo*-inositol is an important precursor to the inositol phosphates including phosphatidylinositol and related phosphoinositides, increasing glucose with increasing *myo*-inositol suggests that membrane rebuilding or enhanced inositol second messenger signalling may contribute to improving cognitive status in some patients. Measurement of CSF energy metabolites may better discern low abundance energy metabolites that are not easily detected or separated by brain imaging techniques. However, a limitation of CSF is that it is not possible to determine the precise brain regions affected. Thus, incorporating CSF metabolic measures with brain imaging may better delineate pathways affected by disease, and predict the trajectory of functional outcomes following intervention. For instance, increased glucose uptake in striatum has been suggested as an early indicator of subclinical neurological involvement [66], but studies in antiretroviral-treated individuals with undetectable viral loads have found varying degrees of reduced glucose uptake in the medial frontal gyrus [67], and evidence for a small but consistent age-related reduction of glucose uptake in the anterior cingulate cortex, but not in other brain regions [68]. Likewise,

creatine, choline, *N*-acetylaspartate, glutamate-containing and glutamine-containing compounds appear to show annual decreases in multiple brain regions of HIV-infected patients on stable cART [69,70]. Neurocognitive decline appears to be specifically associated with reduced glutamate and glutamine containing compounds in multiple brain regions including frontal white and grey matter, basal ganglia and parietal grey matter [69,70]. These disease associated decreases in glutamate and glutamine were correlated with deficits in executive function, motor and psychomotor speed, attention and working memory [14]. Our results support these MRS findings, and further suggest that CSF energy metabolites may contribute critical details useful to identify underlying metabolic alterations associated with changes in cognitive function.

Conclusion

Longitudinal changes in the cognitive status of HIV-infected patients were associated with levels of particular CSF energy metabolites. The patterns of change in these CSF metabolites suggested that worsening cognitive status was associated with increased rates of glycolysis with marked accumulations of the TCA cycle intermediates acetate and citrate. Improving cognitive status was accompanied by a shift to anaerobic glycolysis as evidenced by marked increases of lactate. Future work is required to validate these results and to determine whether CSF energy metabolites could be used as diagnostic or prognostic indicators for HAND, and to further elucidate the underlying mechanisms and cellular implications of these metabolic conversions.

Acknowledgments

Source of funding: These studies were supported by NIH grants R01MH077542, R01MH096636, R03MH103985 to NJH, R01 AG37526 to MMM, and PO1MH075673 to JCM, and by a Capacity Building Studentship to AMD.

References

1. McArthur JC, Hoover D, Bacellar H, Miller E, Cohen B, Becker J, et al. Dementia in AIDS patients incidence and risk factors. Neurology. 1993; 43:2245–12245. [PubMed: 8232937]
2. Cysique LA, Maruff P, Brew BJ. Antiretroviral therapy in HIV infection: are neurologically active drugs important? Arch Neurol. 2004; 61:1699. [PubMed: 15534181]
3. Simioni S, Cavassini M, Annoni J-M, Abraham AR, Bourquin I, Schiffer V, et al. Cognitive dysfunction in HIV patients despite longstanding suppression of viremia. AIDS. 2010; 24:1243–1250. [PubMed: 19996937]
4. Heaton R, Clifford D, Franklin D, Woods S, Ake C, Vaida F, et al. HIV-associated neurocognitive disorders persist in the era of potent antiretroviral therapy CHARTER Study. Neurology. 2010; 75:2087–2096. [PubMed: 21135382]
5. Heaton RK, Franklin DR, Ellis RJ, McCutchan JA, Letendre SL, LeBlanc S, et al. HIV-associated neurocognitive disorders before and during the era of combination antiretroviral therapy: differences in rates, nature, and predictors. J Neurovirol. 2011; 17:3–16. [PubMed: 21174240]
6. McArthur JC, Steiner J, Sacktor N, Nath A. Human immunodeficiency virus-associated neurocognitive disorders: mind the gap. Ann Neurol. 2010; 67:699–714. [PubMed: 20517932]
7. Canestri A, Lescure F-X, Jaureguiberry S, Moulignier A, Amiel C, Marcelin A, et al. Discordance between cerebral spinal fluid and plasma HIV replication in patients with neurological symptoms who are receiving suppressive antiretroviral therapy. Clin Infect Dis. 2010; 50:773–778. [PubMed: 20100092]

8. Kosmiski LA, Ringham BM, Grunwald GK, Bessesen DH. Dual-energy X-ray absorptiometry modeling to explain the increased resting energy expenditure associated with the HIV lipoatrophy syndrome. Am J Clin Nutr. 2009; 90:1525–1531. [PubMed: 19828707]
9. Savage DB, Murgatroyd PR, Chatterjee VK, O'Rahilly S. Energy expenditure and adaptive responses to an acute hypercaloric fat load in humans with lipodystrophy. J Clin Endocrinol Metab. 2005; 90:1446–1452. [PubMed: 15613417]
10. Melchior J-C, Salmon D, Rigaud D, Leport C, Bouvet E, Detruchis P, et al. Resting energy expenditure is increased in stable, malnourished HIV-infected patients. Am J Clin Nutr. 1991; 53:437–441. [PubMed: 1989410]
11. Cade WT, Reeds DN, Overton ET, Herrero P, Waggoner AD, Davila-Roman VG, et al. Effects of human immunodeficiency virus and metabolic complications on myocardial nutrient metabolism, blood flow, and oxygen consumption: a cross-sectional analysis. Cardiovasc Diabetol. 2011; 10:111. [PubMed: 22151886]
12. Reeds DN, Stuart CA, Perez O, Klein S. Adipose tissue, hepatic, and skeletal muscle insulin sensitivity in extremely obese subjects with acanthosis nigricans. Metabolism. 2006; 55:1658–1663. [PubMed: 17142140]
13. Chang E, Sekhar R, Patel S, Balasubramanyam A. Dysregulated energy expenditure in hiv-infected patients: a mechanistic review. Clin Infect Dis. 2007; 44:1509–1517. [PubMed: 17479951]
14. Mohamed MA, Barker PB, Skolasky RL, Selnes OA, Moxley RT, Pomper MG, et al. Brain metabolism and cognitive impairment in HIV infection: a 3-T magnetic resonance spectroscopy study. Magn Reson Imaging. 2010; 28:1251–1257. [PubMed: 20688449]
15. Marcotte T, Deutsch R, Michael B, Franklin D, Cookson D, Bharti A, et al. A concise panel of biomarkers identifies neurocognitive functioning changes in HIV-infected individuals. J Neuroimmune Pharmacol. 2013; 8:1123–1135. [PubMed: 24101401]
16. Borkowski JG, Benton AL, Spreen O. Word fluency and brain damage. Neuropsychologia. 1967; 5:135–140.
17. Reitan, RM.; Davison, LA. Clinical Neuropsychology: current status and applications. Oxford: VH Winston & Sons; 1974.
18. Benedict RH, Schretlen D, Groninger L, Brandt J. Hopkins verbal learning test–revised: normative data and analysis of inter-form and test-retest reliability. Clin Neuropsychol. 1998; 12:43–55.
19. Heaton, RK.; Grant, I.; Matthews, CG. Comprehensive norms for an expanded Halstead-Reitan Battery: demographic corrections, research findings, and clinical applications. Florida: Psychological Assessment Resources Odessa; 1991.
20. Wechsler, D. WAIS-III: Wechsler adult intelligence scale. San Antonio: Psychological Corporation; 1997.
21. Diehr MC, Heaton RK, Miller W, Grant I. The Paced Auditory Serial Addition Task (PASAT): norms for age, education, and ethnicity. Assessment. 1998; 5:375–387. [PubMed: 9835661]
22. Kløve, H. Grooved pegboard. Indiana: Lafayette Instruments; 1963.
23. Wishart DS, Jewison T, Guo AC, Wilson M, Knox C, Liu Y, et al. HMDB3. 0: the Human Metabolome database in 2013. Nucleic Acids Res. 2013; 41:D801–D807. [PubMed: 23161693]
24. Wishart DS, Knox C, Guo AC, Eisner R, Young N, Gautam B, et al. HMDB: a knowledgebase for the human metabolome. Nucleic Acids Res. 2009; 37:D603. [PubMed: 18953024]
25. Wishart DS, Tzur D, Knox C, Eisner R, Guo AC, Young N, et al. HMDB: the Human Metabolome database. Nucleic Acids Res. 2007; 35:D521–D526. [PubMed: 17202168]
26. Waterman C, Currie R, Cottrell L, Dow J, Wright J, Waterfield C, et al. An integrated functional genomic study of acute phenobarbital exposure in the rat. BMC Genomics. 2010; 11:9. [PubMed: 20053287]
27. Breiman, L.; Friedman, JH.; Olshen, RA.; Stone, CJ. Classification and regression trees. Wadsworth International Group; 1984.
28. Erbsloh F, Bernsmeier A, Hillesheim H. The glucose consumption of the brain & its dependence on the liver. Arch Psychiatr Nervenkr Z Gesamte Neurol Psychiatr. 1958; 196:611–626. [PubMed: 13534602]
29. Deelchand DK, Shestov AA, Koski DM, Uğurbil K, Henry P-G. Acetate transport and utilization in the rat brain. J Neurochem. 2009; 109:46–54. [PubMed: 19393008]

30. Muir D, Berl S, Clarke DD. Acetate and fluoroacetate as possible markers for glial metabolism in vivo. Brain Res. 1986; 380:336–340. [PubMed: 3756485]
31. Blüml S, Panigrahy A, Laskov M, Dhall G, Krieger MD, Nelson MD, et al. Elevated citrate in pediatric astrocytomas with malignant progression. Neurooncology. 2011; 13:1107–1117.
32. Blum H, Balschi J, Johnson R. Coupled in vivo activity of creatine phosphokinase and the membrane-bound (Na+, K+)-ATPase in the resting and stimulated electric organ of the electric fish Narcine brasiliensis. J Biol Chem. 1991; 266:10254–10259. [PubMed: 1645345]
33. Saks V, Rosenshtraukh L, Smirnov V, Chazov E. Role of creatine phosphokinase in cellular function and metabolism. Can J Physiol Pharmacol. 1978; 56:691–706. [PubMed: 361188]
34. Schuenke K, Gelman BB. Human microglial cell isolation from adult autopsy brain: brain pH, regional variation, and infection with human immunodeficiency virus type 1. J Neurovirol. 2003; 9:346–357. [PubMed: 12775418]
35. Kure K, Lyman WD, Weidenheim KM, Dickson DW. Cellular localization of an HIV-1 antigen in subacute AIDS encephalitis using an improved double-labeling immunohistochemical method. Am J Pathol. 1990; 136:1085. [PubMed: 1693470]
36. Jordan CA, Watkins BA, Kufta C, Dubois-Dalcq M. Infection of brain microglial cells by human immunodeficiency virus type 1 is CD4 dependent. J Virol. 1991; 65:736–742. [PubMed: 1702842]
37. McArthur JC, Brew BJ, Nath A. Neurological complications of HIV infection. Lancet Neurol. 2005; 4:543–555. [PubMed: 16109361]
38. Churchill MJ, Wesselingh SL, Cowley D, Pardo CA, McArthur JC, Brew BJ, et al. Extensive astrocyte infection is prominent in human immunodeficiency virus: associated dementia. Ann Neurol. 2009; 66:253–258. [PubMed: 19743454]
39. Dewhurst S, Bresser J, Stevenson M, Sakai K, Evinger-Hodges MJ, Volsky DJ. Susceptibility of human glial cells to infection with human immunodeficiency virus (HIV). FEBS Lett. 1987; 213:138–143. [PubMed: 3549356]
40. Ranki A, Nyberg M, Ovod V, Haltia M, Elovaara I, Raininko R, et al. Abundant expression of HIV Nef and Rev proteins in brain astrocytes invivo is associated with dementia. AIDS. 1995; 9:1001–1008. [PubMed: 8527071]
41. Fiala M, Rhodes RH, Shapshak P, Nagano I, Martinez-maza O, Diagne A, et al. Regulation of HIV-1 infection in astrocytes: expression of Nef, TNF-α and IL-6 is enhanced in coculture of astrocytes with macrophages. J Neurovirol. 1996; 2:158–166. [PubMed: 8799208]
42. Janabi N, Di Stefano M, Wallon C, Hery C, Chiodi F, Tardieu M. Induction of human immunodeficiency virus type 1 replication in human glial cells after proinflammatory cytokines stimulation: effect of IFNγ, IL1β, and TNFα on differentiation and chemokine production in glial cells. Glia. 1998; 23:304–315. [PubMed: 9671961]
43. Saito Y, Sharer L, Epstein L, Michaels J, Mintz M, Louder M, et al. Overexpression of nef as a marker for restricted HIV-1 infection of astrocytes in postmortem pediatric central nervous tissues. Neurology. 1994; 44:474–1474. [PubMed: 8145918]
44. Nath A, Hartloper V, Furer M, Fowke KR. Infection of human fetal astrocytes with HIV-1: viral tropism and the role of cell to cell contact in viral transmission. J Neuropathol Exp Neurol. 1995; 54:320–330. [PubMed: 7745431]
45. McCarthy M, He J, Wood C. HIV-1 strain-associated variability in infection of primary neuroglia. J Neurovirol. 1998; 4:80–89. [PubMed: 9531014]
46. Starling I, Wright A, Arbuthnott G, Harkiss G. Acute in vivo neurotoxicity of peptides from Maedi Visna virus transactivating protein Tat. Brain Res. 1999; 830:285–291. [PubMed: 10366685]
47. Gjedde A, Marrett S. Glycolysis in neurons, not astrocytes, delays oxidative metabolism of human visual cortex during sustained checkerboard stimulation in vivo. J Cereb Blood Flow Metab. 2001; 21:1384–1392. [PubMed: 11740199]
48. Ellis RJ, Badiee J, Vaida F, Letendre S, Heaton RK, Clifford D, et al. CD4 nadir is a predictor of HIV neurocognitive impairment in the era of combination antiretroviral therapy. AIDS. 2011; 25:1747–1751. [PubMed: 21750419]
49. Cysique LA, Murray JM, Dunbar M, Jeyakumar V, Brew BJ. A screening algorithm for HIV-associated neurocognitive disorders. HIV Med. 2010; 11:642–649. [PubMed: 20456505]

50. Wyss MT, Jolivet R, Buck A, Magistretti PJ, Weber B. In vivo evidence for lactate as a neuronal energy source. J Neurosci. 2011; 31:7477–7485. [PubMed: 21593331]
51. Pellerin L, Magistretti PJ. Sweet sixteen for ANLS. J Cereb Blood Flow Metab. 2011; 32:1152–1166. [PubMed: 22027938]
52. Patel AB, Lai JC, Chowdhury GM, Hyder F, Rothman DL, Shulman RG, et al. Direct evidence for activity-dependent glucose phosphorylation in neurons with implications for the astrocyte-to-neuron lactate shuttle. Proc Natl Acad Sci. 2014; 111:5385–5390. [PubMed: 24706914]
53. Pellerin L, Magistretti PJ. Glutamate uptake into astrocytes stimulates aerobic glycolysis: a mechanism coupling neuronal activity to glucose utilization. Proc Natl Acad Sci. 1994; 91:10625–10629. [PubMed: 7938003]
54. Bittar PG, Charnay Y, Pellerin L, Bouras C, Magistretti PJ. Selective distribution of lactate dehydrogenase isoenzymes in neurons and astrocytes of human brain. J Cereb Blood Flow Metab. 1996; 16:1079–1089. [PubMed: 8898679]
55. Pellerin L, Magistretti P. Excitatory amino acids stimulate aerobic glycolysis in astrocytes via an activation of the Na+/K+ ATPase. Dev Neurosci. 1996; 18:336–342. [PubMed: 8940604]
56. Dienel GA. Brain lactate metabolism: the discoveries and the controversies. J Cereb Blood Flow Metab. 2011; 32:1107–1138. [PubMed: 22186669]
57. Yang J, Ruchti E, Petit J-M, Jourdain P, Grenningloh G, Allaman I, et al. Lactate promotes plasticity gene expression by potentiating NMDA signaling in neurons. Proc Natl Acad Sci. 2014; 111:12228–12233. [PubMed: 25071212]
58. Tang F, Lane S, Korsak A, Paton J, Gourine A, Kasparov S, et al. Lactate-mediated glia-neuronal signalling in the mammalian brain. Nat Commun. 2014; 5:3284. [PubMed: 24518663]
59. Fernandes S, Edwards T, Ng K, Robinson S. HIV-1 protein gp120 rapidly impairs memory in chicks by interrupting the glutamate–glutamine cycle. Neurobiol Learn Mem. 2007; 87:1–8. [PubMed: 16714124]
60. Vartak-Sharma N, Gelman BB, Joshi C, Borgmann K, Ghorpade A. Astrocyte elevated gene-1 is a novel modulator of HIV-1-associated neuroinflammation via regulation of nuclear factor-κB signaling and excitatory amino acid transporter-2 repression. J Biol Chem. 2014; 289:19599–19612. [PubMed: 24855648]
61. Visalli V, Muscoli C, Sacco I, Sculco F, Palma E, Costa N, et al. N-acetylcysteine prevents HIV gp 120-related damage of human cultured astrocytes: correlation with glutamine synthase dysfunction. BMC Neurosci. 2007; 8:106. [PubMed: 18062818]
62. Cohen RA, Harezlak J, Gongvatana A, Buchthal S, Schifitto G, Clark U, et al. Cerebral metabolite abnormalities in human immunodeficiency virus are associated with cortical and subcortical volumes. J Neurovirol. 2010; 16:435–444. [PubMed: 20961212]
63. Cysique LA, Moffat K, Moore DM, Lane TA, Davies NW, Carr A, et al. HIV, vascular and aging injuries in the brain of clinically stable HIV-infected adults: a 1H MRS study. PLoS One. 2013; 8:e61738. [PubMed: 23620788]
64. Chang L, Lee P, Yiannoutsos C, Ernst T, Marra C, Richards T, et al. A multicenter in vivo proton-MRS study of HIV-associated dementia and its relationship to age. Neuroimage. 2004; 23:1336–1347. [PubMed: 15589098]
65. Cassol E, Misra V, Holman A, Kamat A, Morgello S, Gabuzda D. Plasma metabolomics identifies lipid abnormalities linked to markers of inflammation, microbial translocation, and hepatic function in HIV patients receiving protease inhibitors. BMC Infect Dis. 2013; 13:203. [PubMed: 23641933]
66. Rottenberg DA, Sidtis JJ, Strother SC, Schaper KA, Anderson JR, Nelson MJ, et al. Abnormal cerebral glucose metabolism in HIV-1 seropositive subjects with and without dementia. J Nucl Med. 1996; 37:1133–1141. [PubMed: 8965184]
67. Andersen ÅB, Law I, Krabbe KS, Bruunsgaard H, Ostrowski SR, Ullum H, et al. Cerebral FDG-PET scanning abnormalities in optimally treated HIV patients. J Neuroinflammation. 2010; 7:13. [PubMed: 20152054]
68. Towgood KJ, Pitkanen M, Kulasegaram R, Fradera A, Soni S, Sibtain N, et al. Regional cerebral blood flow and FDG uptake in asymptomatic HIV-1 men. Hum Brain Mapp. 2013; 34:2484–2493. [PubMed: 22496057]

69. Ernst T, Jiang CS, Nakama H, Buchthal S, Chang L. Lower brain glutamate is associated with cognitive deficits in HIV patients: a new mechanism for HIV-associated neurocognitive disorder. J Magn Reson Imaging. 2010; 32:1045–1053. [PubMed: 21031507]

70. Gongvatana A, Harezlak J, Buchthal S, Daar E, Schifitto G, Campbell T, et al. Progressive cerebral injury in the setting of chronic HIV infection and antiretroviral therapy. J Neurovirol. 2013; 19:209–218. [PubMed: 23613008]

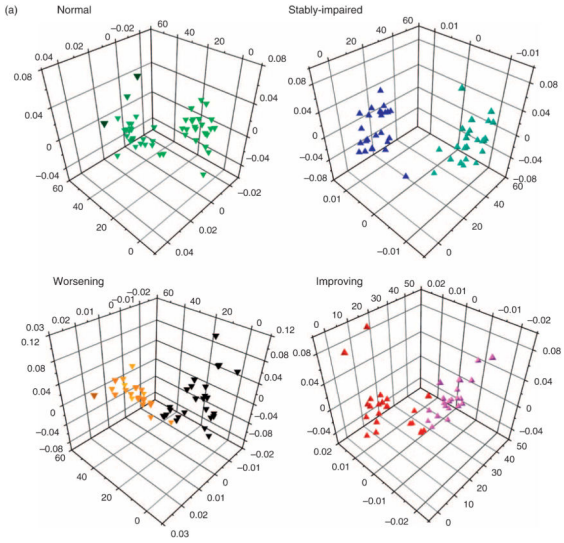

(b)

Model	q^2	Positive metabolites		
Normal	0.61	Citric acid	Pyroglutamic acid	
Stably-impaired	0.84	Glutamine	Glucose	Oxalacetic acid
Worsening	0.47	Citric acid	Pyroglutamic acid	
Improving	0.52	Glutamine	Glucose	

(c)

Model	q^2	Negative metabolites		
Normal	0.61	Glutamine	Lactic acid	
Stably-impaired	0.84	Citric acid	Lactic acid	Pyroglutamic acid Myoinositol
Worsening	0.47	Glutamine	Lactic acid	
Improving	0.52	Citric acid	Pyroglutamic acid	Lactic acid

Fig. 1. Multivariate analyses of cerebrospinal fluid energy metabolites separate temporal changes in cognitive status

(a) Three-dimensional PLS-DA plots demonstrating significant ($q^2 < 0.4$) longitudinal separation in each of four neurocognitive states examined: Worsening visit one (black), visit two (yellow); Normal visit one (light green), visit two (dark green); Improving visit one (red); visit two (pink); and stably impaired visit one (blue), visit two (light blue). Imbedded table shows metabolites that were (b) elevated at the first visit compared with the second visit, and (c) reduced at the first visit compared with the second visit.

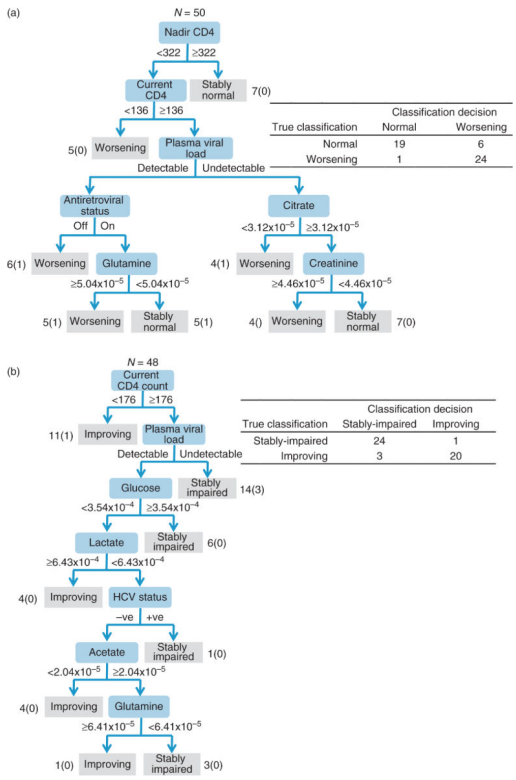

Fig. 2. A combination of metabolites and clinical features generates prognostic models for worsening and improving cognitive function

Recursive partitioning model and confusion matrix showing prognostic markers for (a) worsening and (b) improving cognitive status. Each node in a matrix shows the variable (clinical parameter or metabolite), and the cut-off value for each variable for the assignment to worsening, improving, normal or stably impaired. Boxes in grey show classification decisions and adjacent values are the number of patients correctly and incorrectly classified (incorrectly classified are shown in parenthesis). The worsening model produced a predictive accuracy of 86%, sensitivity of 96%, and specificity of 76%. The improving model produced an accuracy of 92%, sensitivity of 87%, and specificity of 96%.

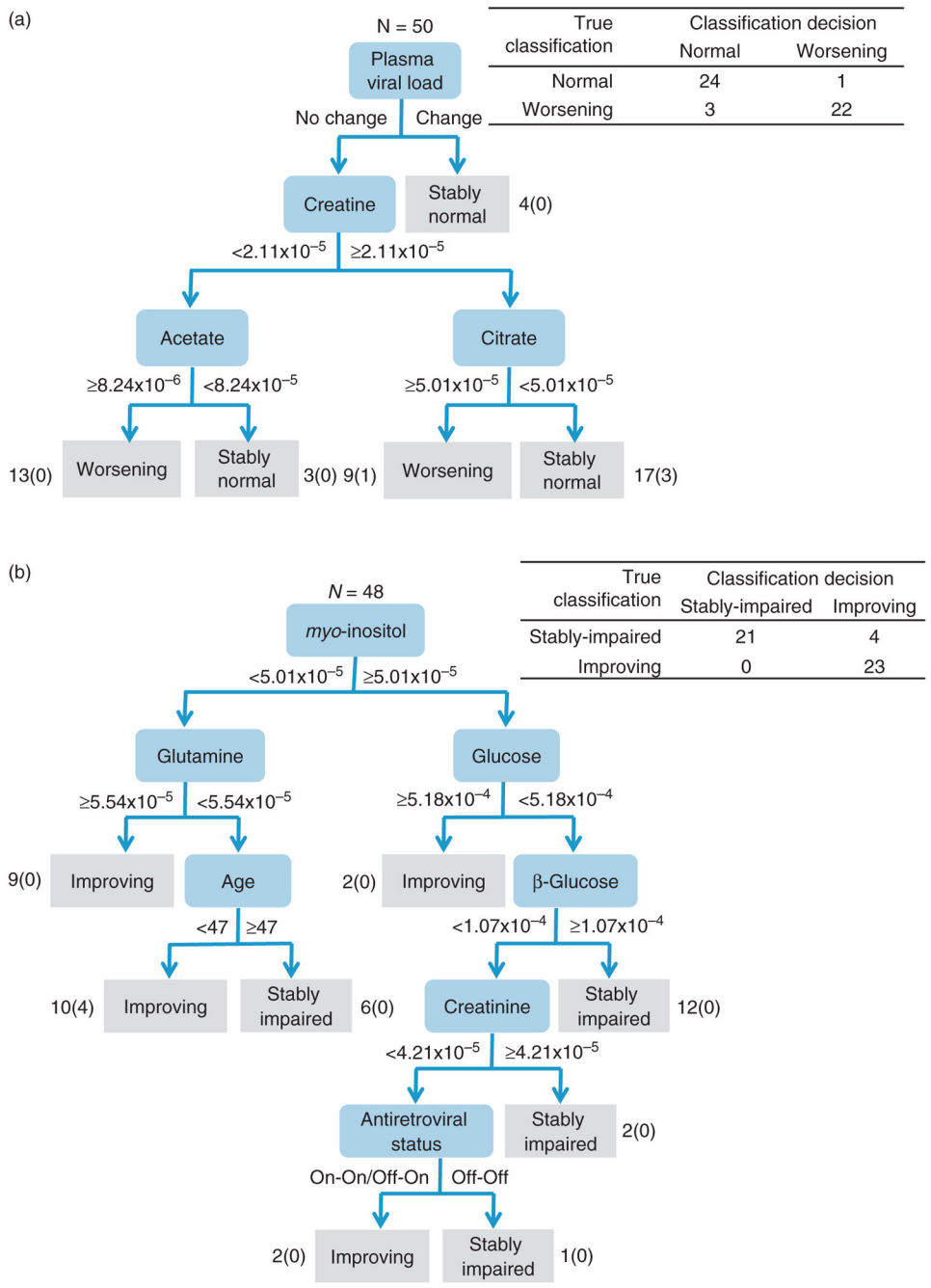

Fig. 3. Prognostic models for cognitive improvement and worsening generated using longitudinal changes in metabolites and clinical features

Recursive partitioning model and confusion matrix showing prognostic markers for (a) worsening, and (b) improving cognitive status generated using visit one cerebrospinal fluid metabolites and change in clinical parameters from visit one to visit two. Nodes show the variable (clinical parameter or metabolite) and the cut-off value for change in each variable for assignment to improving, stably impaired, or normal. Boxes in grey show classification decisions and adjacent values are the number of patients correctly and incorrectly classified (incorrectly classified are shown in parenthesis). The worsening model produced an

accuracy of 92%, sensitivity of 88%, and specificity of 96%. The improving model has a total accuracy of 92% with a sensitivity of 100%, and specificity of 84%.

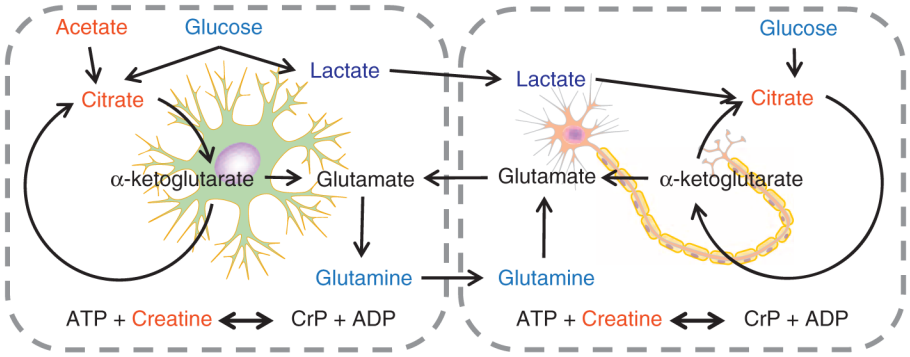

Fig. 4. Summary diagram demonstrating the key CSF metabolite changes found to occur during worsening (highlighted in red) and improving (highlighted in blue) cognitive status

ADP,; ATP,; CrP,.

Table 1

Cross-sectional associations between the cerebrospinal fluid metabolites and domain specific *t* scores at baseline among all patients (*n* = 97).

	Global		Verbal		Executive functioning		Speed of information processing		Learning		Recall		Working memory		Motor	
	b	***P***	***b***	***P***	***b***	***P***	***b***	***P***	***b***	***P***	***b***	***P***	***b***	***P***	***b***	***P***
Lactate	−3.28	0.10	−1.19	0.68	***−6.88***	***0.04***	−1.06	0.69	−4.07	0.18	−4.70	0.12	0.70	0.76	***−7.68***	***0.03***
Glutamine	−0.03	0.99	0.20	0.95	0.09	0.98	1.30	0.67	0.58	0.87	−0.13	0.97	2.21	0.40	−5.76	0.15
Pyroglutamate	***−1.95***	***0.05***	0.67	0.64	***−3.73***	***0.02***	−0.82	0.53	***−3.45***	***0.02***	***−3.55***	***0.02***	−0.12	0.92	*−3.12*	*0.07*
Citrate	***−3.61***	***0.03***	−2.50	0.31	***−5.67***	***0.04***	−1.93	0.39	−3.62	0.16	−4.60	0.07	−2.67	0.16	***−7.18***	***0.01***
Creatine	***−3.85***	***0.02***	−0.71	0.77	***−6.55***	***0.02***	−2.00	0.37	*−4.91*	*0.05*	***−6.00***	***0.02***	−1.78	0.34	*−5.33*	*0.06*
Creatinine	−2.49	0.14	0.77	0.75	−4.12	0.14	−0.67	0.77	−3.09	0.23	−3.93	0.12	−0.45	0.82	***−7.11***	***0.01***
Glucose	−2.66	0.19	−1.09	0.71	*−5.69*	*0.09*	0.85	0.75	−4.88	0.11	*−5.68*	*0.06*	−0.28	0.90	−5.28	0.13
Myo-inositol	*−2.82*	*0.08*	0.12	0.96	*−4.78*	*0.07*	−0.63	0.77	*−4.65*	*0.06*	***−4.76***	***0.05***	0.25	0.89	***−6.08***	***0.03***
β-glucose	−2.78	0.17	−1.49	0.61	*−5.67*	*0.09*	1.01	0.71	−4.76	0.12	*−5.59*	*0.07*	−0.29	0.90	−5.65	0.11
Alanine	***−3.82***	***0.03***	−1.98	0.43	*−5.44*	*0.06*	−3.40	0.14	−3.97	0.13	***−5.28***	***0.04***	−0.08	0.97	***−7.01***	***0.02***
Acetate	*−2.80*	*0.06*	−0.30	0.89	*−4.73*	*0.06*	−1.78	0.38	−3.44	0.13	***−4.44***	***0.05***	0.10	0.95	***−5.25***	***0.04***

All models control for age, education, nadir $CD4^+$ cell count and cerebrospinal fluid storage time. b = β-coefficient. Numbers in bold indicate $P<0.05$. Numbers in italics indicate $P<0.10$.